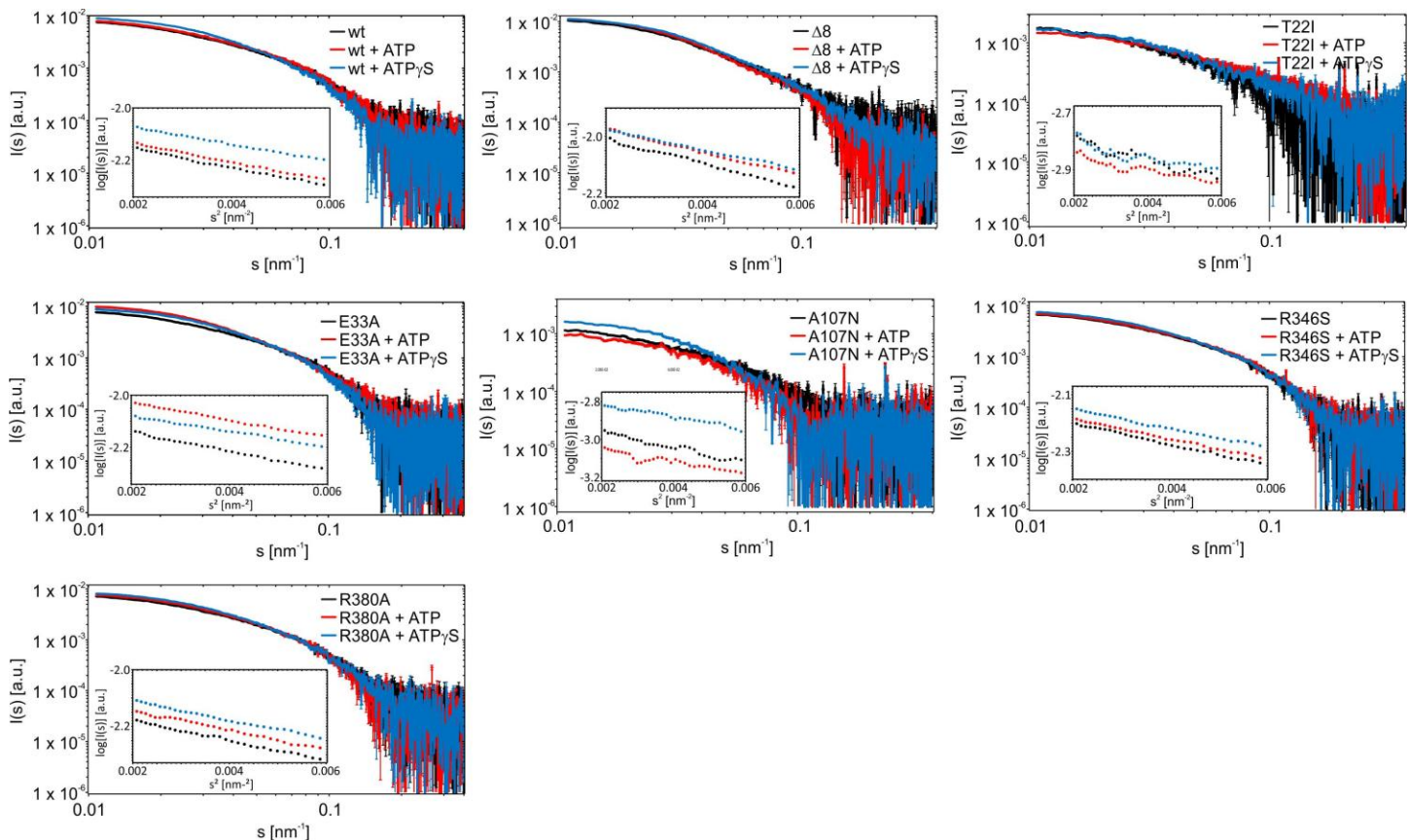


Supplementary Figure 1

In vivo control experiments.

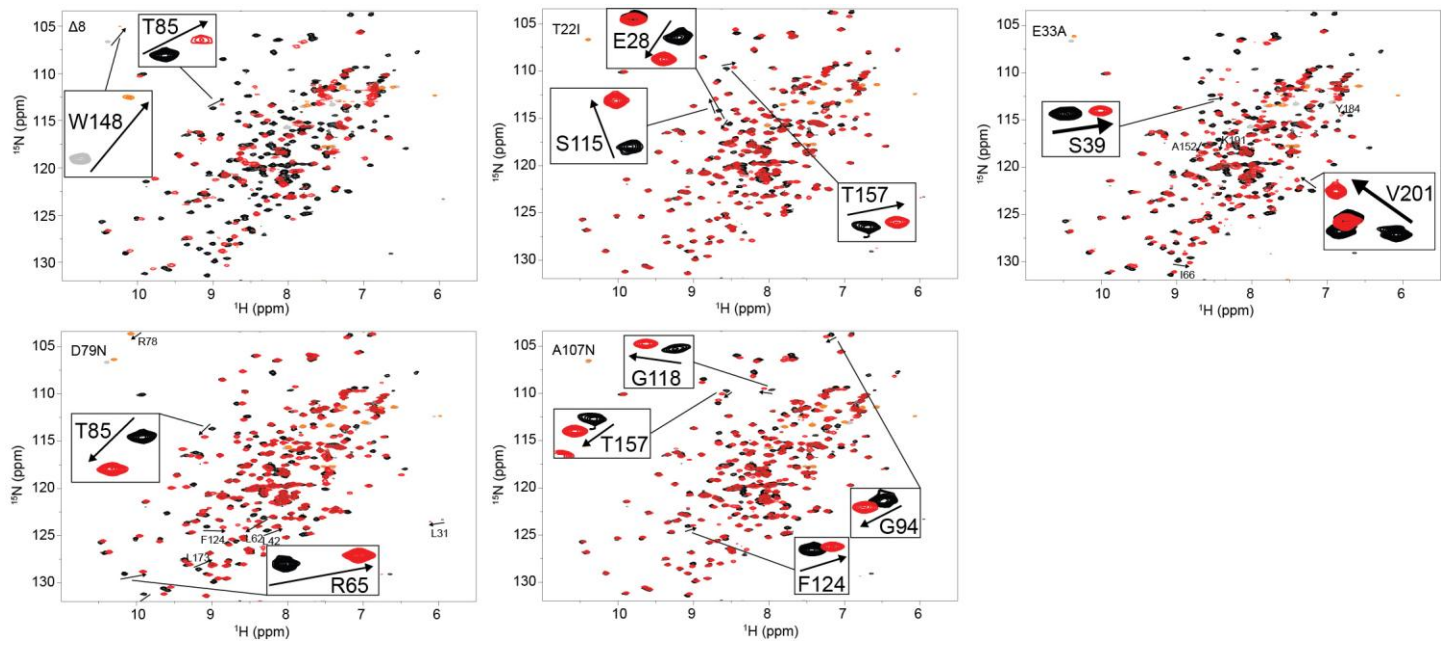
(a) Test for plasmid loss. Yeast cells were streaked out on media lacking uracil after 5'FOA shuffling. As control non shuffled cells expressing Hsp90 wt (pKAT6) were used. (b) Tetrad analysis was performed with p415-GPD-HSP82^{E33A} or the empty vector (ev) as control. The resulted Hsp90 double knock-out strain is complemented by Hsp90 variant E33A (left panel) whereas the empty vector p415GPD was not able to support growth of the double knock-out as always one spore is inviable (right panel). The distributions of the kanMX cassette show tetra type (TT) distribution in the E33A complemented strain, always one out of four spores must carry a genomic double knock-out of Hsp90. In the vector control only two spores are G418 resistant confirming that the deletion of both Hsp90 alleles is lethal when Hsp90 is not provided by a plasmid. (c) 5'FOA Shuffling approach was carried out with different yeast shuffling strains and under GPD- and endogenous promotor. In all strains Hsp90 variant E33A supports yeast cell growth.



Supplementary Figure 2

SAXS scattering curves.

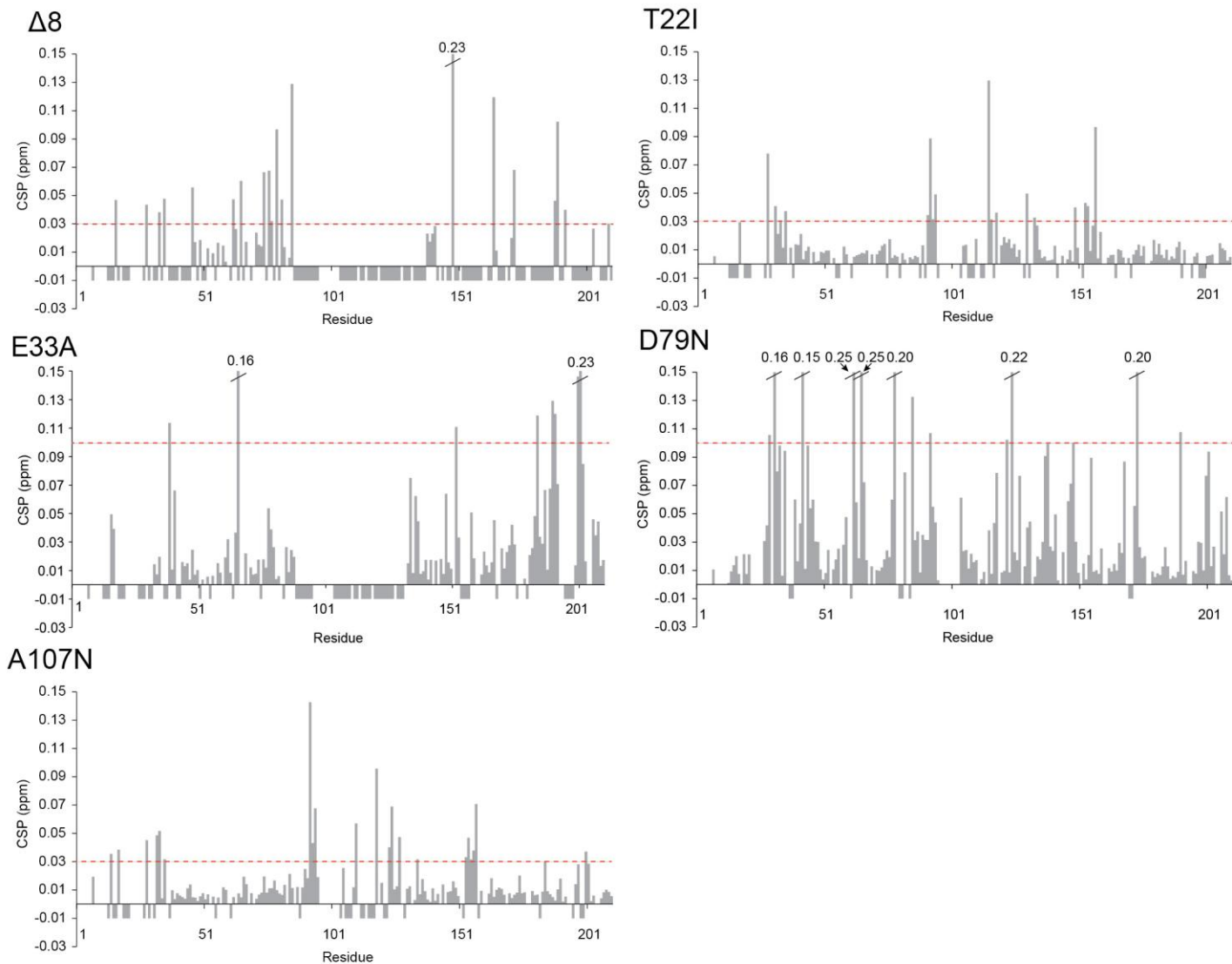
Experimental X-ray scattering data of Hsp90 versions recorded at different sample concentrations. Both the s , and $I(s)$ axes are shown in a logarithmic representation. The angular ranges from $0.0012 - 0.4 \text{ nm}^{-1}$ are compared.



Supplementary Figure 3

^1H - ^{15}N -HSQC spectra of the Hsp90 N-domain mutants.

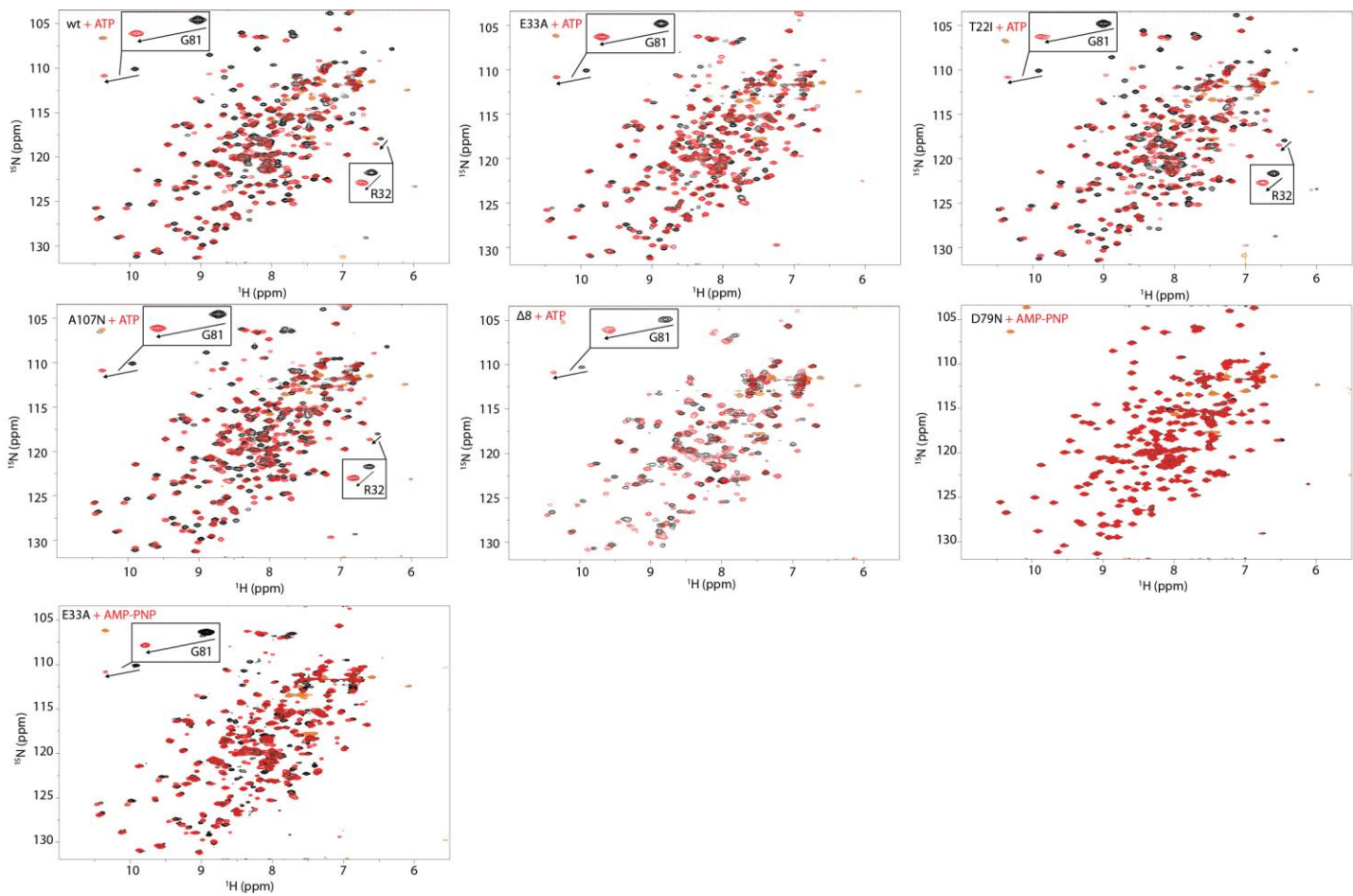
^1H - ^{15}N -HSQC spectra of the indicated mutant (red) are superposed with spectra of the wildtype (black) of the N-terminal domain of yeast Hsp90. Negative peaks are plotted in orange and grey respectively. Examples of strongly shifting peaks are highlighted in boxes.



Supplementary Figure 4

Chemical-shift-perturbation plots of the Hsp90 N-domain mutants.

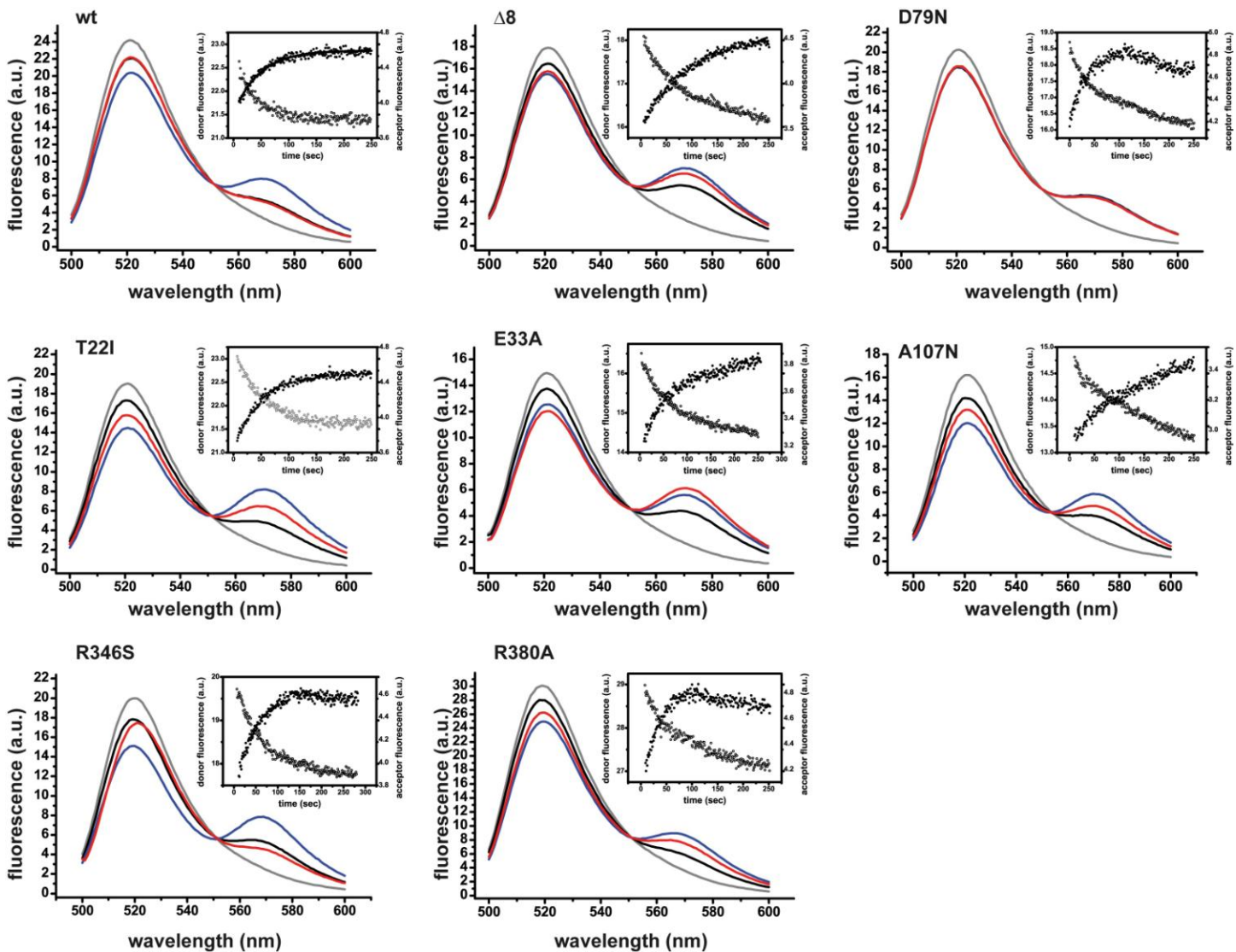
Chemical shift perturbation of the $^1\text{H}, ^{15}\text{N}$ -HSQC spectra from Supplementary Figure 3 between the indicated mutant and the wildtype of the N-terminal domain of yeast Hsp90. Negative chemical shifts indicate shifting residues that could not be assigned in the complex. Residues which are not assigned in the wildtype are indicated by gaps. Chemical shift changes larger than 0.15 ppm are indicated on top of the bars. The red lines indicate the cut-off values used in Figure 2.



Supplementary Figure 5

^1H , ^{15}N -HSQC spectra of the Hsp90 N-domain mutants in complex with nucleotide.

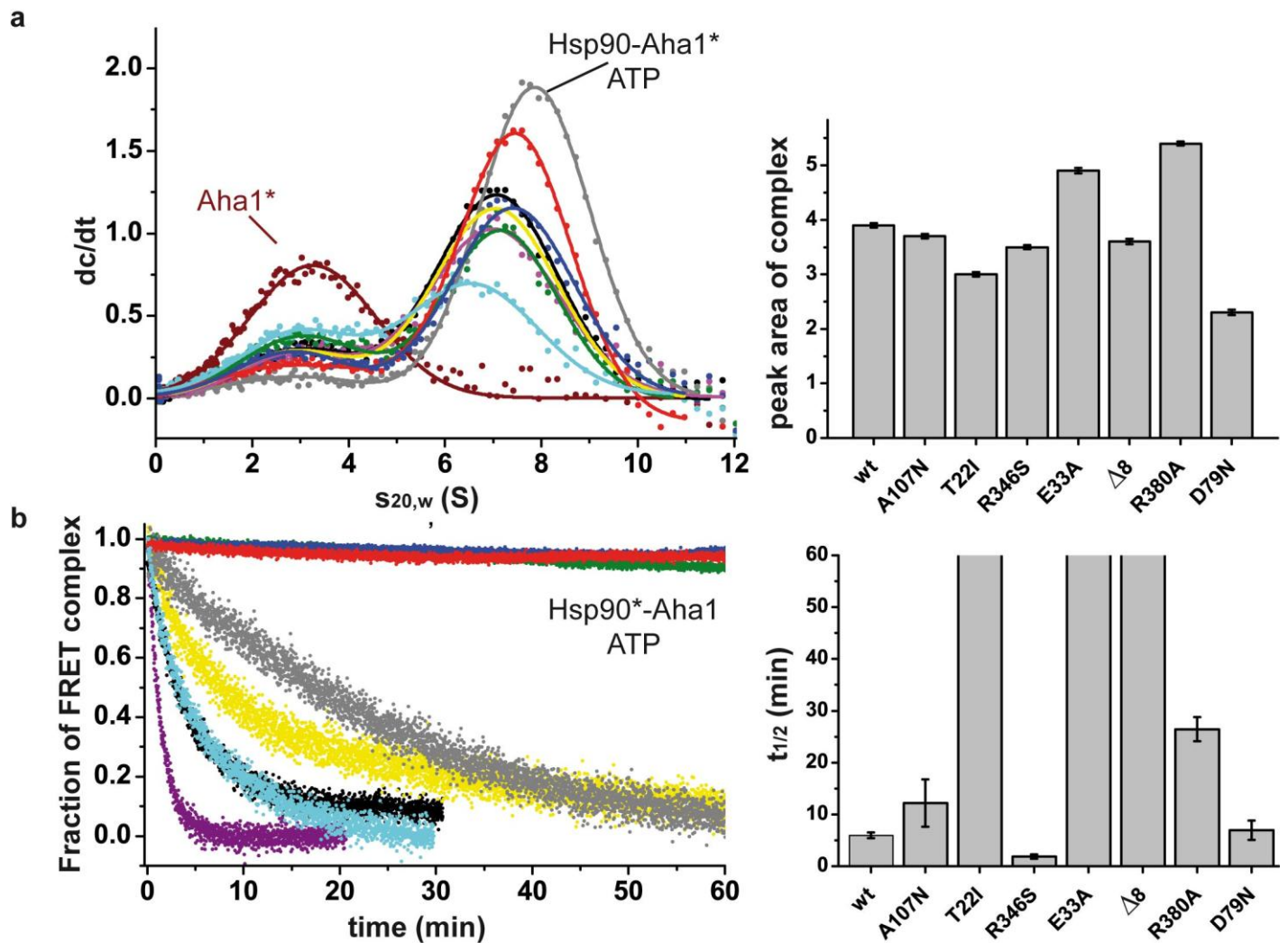
^1H , ^{15}N -HSQC spectra of the indicated variant of the N-terminal domain of yeast Hsp90 with (red) and without (black) the indicated nucleotide are superposed. Negative peaks are plotted in orange and grey respectively. Examples of strongly shifting peaks are highlighted in boxes.



Supplementary Figure 6

Fluorescence spectra of the N- and M-domain labeled Hsp90 heterocomplex in the absence or presence of nucleotides.

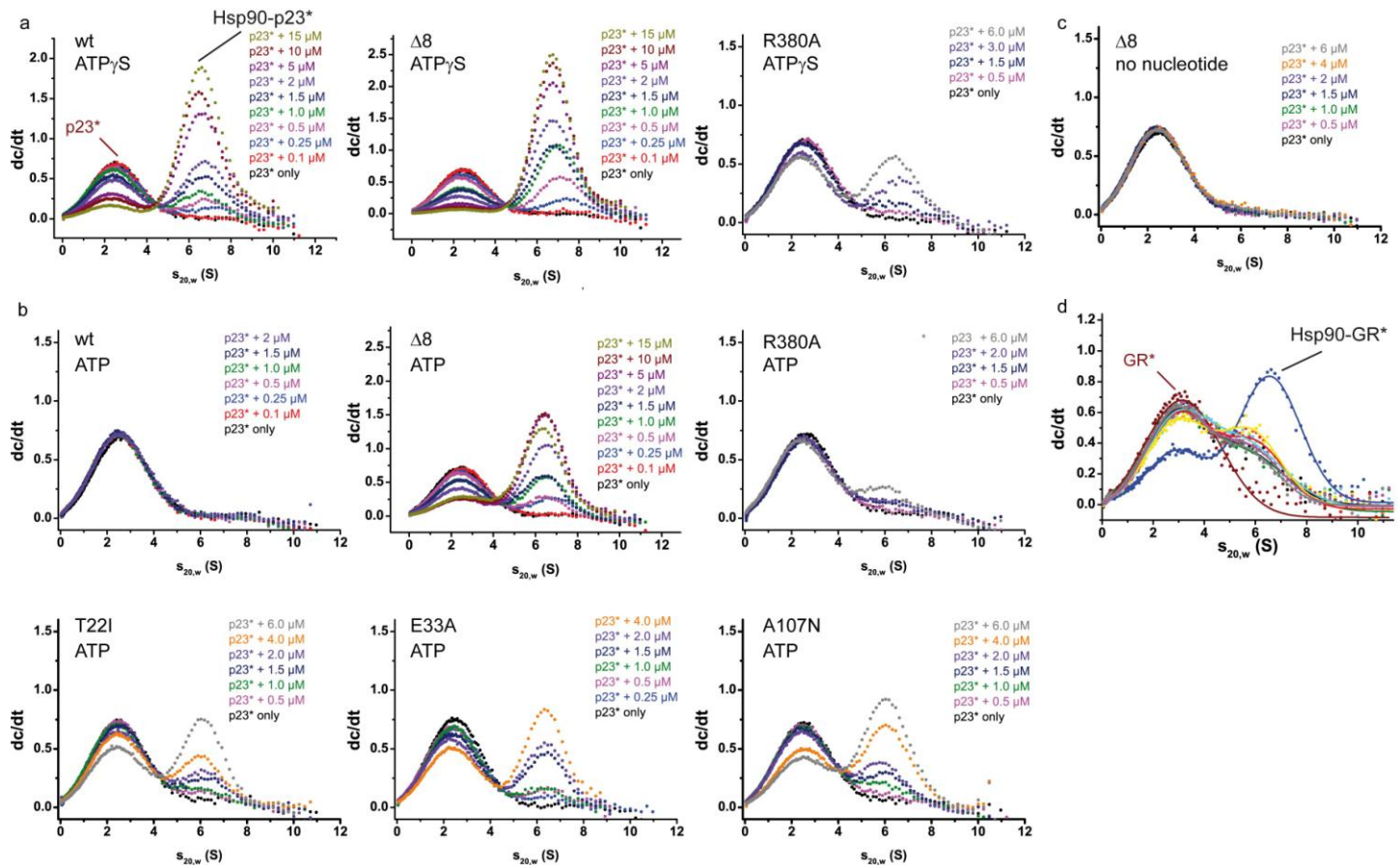
The inset indicates the subunit exchange of the Hsp90 variants. Decrease in donor channel and increase in acceptor channel fluorescence were monitored and indicate FRET (inset). Following fluorescence spectra were recorded: donor only (grey), Hsp90 hetero-complex without nucleotide (black), in the presence of ATP (red) and ATP γ S (blue).



Supplementary Figure 7

Hsp90-Aha1 interaction *in vitro*.

(a) The binding of the labeled co-chaperone Aha1* to different Hsp90 mutants in the presence of ATP monitored by analytical ultracentrifugation with fluorescence detection and derived from dc/dt plots (left panel). Following color code is used: Aha1* in brown, Aha1* in complex with: wt in black, A107N in yellow, Δ8 in blue, T22I in green, R346S in purple, R380A in grey, E33A in red and D79N in light blue. The areas of the Hsp90-Aha1* complex peaks in presence of 2 mM ATP (right panel). Error bars indicate standard error of the fit. (b) N-terminal dimerization stability of the Hsp90 variants in presence of ATP and Aha1. FRET chase experiments were performed with preformed Hsp90 FRET-complexes in the presence of ATP and the co-chaperone Aha1. The chase was induced by addition of 20-fold excess of the unlabeled Hsp90 D79N and the disruption of complex was monitored by following the decrease in acceptor fluorescence. Apparent half-lives ($t_{1/2}$) were derived from a non-linear fit of the acceptor signal changes. Means of technical replicates are shown. Error bars indicate s.d. (n value=3).



Supplementary Figure 8

Nucleotide-dependent Hsp90-p23 and Hsp90-GR interactions *in vitro*.

Hsp90 variants were titrated with increasing amounts of fluorescein-labeled p23*. The binding of p23 to different Hsp90 mutants in the presence of (a) 2 mM ATP γ S, (b) 2 mM ATP and (c) without nucleotide were monitored by analytical ultracentrifugation with a fluorescence detection unit and derived from dc/dt plots. (d) The binding of labeled GR* to different Hsp90 mutants in the absence of nucleotide were monitored by analytical ultracentrifugation and derived from dc/dt plots. Following color code is used: GR* in brown, GR* in complex with: wt in black, A107N in yellow, Δ8 in blue, T22I in green, R346S in purple, R380A in grey, E33A in red and D79N in light blue.

Supplementary Table 1. ATPase activity of Hsp90 variants and its activation by the co-chaperone Aha1. Means of technical replicates are shown, error bars indicate s.d. (n value =3).

Hsp90 variant	ATPase activity			Aha1 stimulation			
	k_{cat} (min ⁻¹)	K_M (mM)	k_{cat}/K_M	K_{Dapp} (μM)	V_{max} (min ⁻¹)	(xfold)	V_{max}/K_{Dapp}
wt	0.55 ± 0.02	0.32	1.72	6.8 ± 0.7	12.9 ± 0.4	23	1.9
Δ8	1.13 ± 0.05	0.07	16.14	1.3 ± 0.1	7.2 ± 0.1	6	5.5
T22I	0.85 ± 0.08	0.14	6.07	5.3 ± 0.9	5.1 ± 0.2	6	1.0
E33A	< 0.001	-	-	-	< 0.001	0	-
D79N	< 0.001	-	-	-	< 0.001	0	-
A107N	2.14 ± 0.08	0.01	21.40	3.7 ± 0.4	23.1 ± 0.4	11	6.2
R346S	0.17 ± 0.02	0.20	0.85	7.0 ± 1.0	13.4 ± 0.3	79	1.9
R380A	0.18 ± 0.06	0.36	0.50	2.1 ± 0.7	0.36 ± 0.02	2	0.2

Supplementary Table 2. SAXS data and analysis. Means of technical replicates are shown, error bars indicate s.d. (n value =3).

Sample	w/o nucleotide			ATP			ATPγS		
	R _g [Å]	D _{max} [Å]	Molecular mass [kDa]*	R _g [Å]	D _{max} [Å]	Molecular mass [kDa]*	R _g [Å]	D _{max} [Å]	Molecular mass [kDa]*
Hsp90	64.2 ± 0.2	240	173	58.3 ± 0.1	220	185	53.5 ± 0.2	170	181
⊗8	61.9 ± 0.4	240	164	61.2 ± 0.1	220	164	55.6 ± 0.2	190	164
T22I	69.3 ± 0.5	240	186	55.9 ± 0.2	220	180	52.0 ± 0.4	180	170
E33A	64.3 ± 0.7	260	171	58.7 ± 0.1	220	176	53.8 ± 0.2	180	162
A107N	68.0 ± 0.4	220	165	54.5 ± 0.4	220	167	55.1 ± 0.4	180	167
R346S	70.1 ± 0.2	240	162	65.3 ± 0.2	220	175	63.1 ± 0.2	220	184
R380A	68.7 ± 0.2	240	184	62.6 ± 0.1	220	179	61.1 ± 0.2	220	183

*The molecular mass was determined using Porod's law.

Supplementary Table 3: Rate constants of FRET complex formation and nucleotide-induced conformational changes of Hsp90 variants. Means of technical replicates are shown, error bars indicate s.d. (n value =3).

Hsp90 variant	FRET complex formation subunit exchange	nucleotide-induced closing kinetics	
	k_{se} (s ⁻¹)	k_{app} (ATP γ S) (min ⁻¹)	k_{app} (ATP) (min ⁻¹)
wt	0.019 ± 0.002	0.41 ± 0.07	---
Δ8	0.014 ± 0.002	0.87 ± 0.23	1.63 ± 0.14
T22I	0.028 ± 0.008	0.97 ± 0.19	1.34 ± 0.32
E33A	0.036 ± 0.009	0.40 ± 0.06	0.25 ± 0.05
D79N	0.014 ± 0.003	---	---
A107N	0.011 ± 0.006	0.90 ± 0.20	4.60 ± 1.09
R346S	0.041 ± 0.004	0.15 ± 0.02	---
R380A	0.020 ± 0.011	0.16 ± 0.03	0.22 ± 0.02

--- no change in acceptor fluorescence signal observed

Supplementary Table 4. Apparent half-lives ($t_{1/2}$) of Hsp90 complexes without nucleotide and in the presence of different nucleotides and co-chaperones determined by FRET chase experiments. Means of technical replicates are shown, error bars indicate s.d. (n value =3).

Hsp90 variant	$t_{1/2}$ (min) no nucleotide	$t_{1/2}$ (min) ATP	$t_{1/2}$ (min) Sba1/ATP	$t_{1/2}$ (min) Aha1/ATP	$t_{1/2}$ (min) ATP γ S
wt	0.67 ± 0.25	0.82 ± 0.28	1.03 ± 0.09	5.96 ± 0.53	41.53 ± 4.84
$\Delta 8$	0.87 ± 0.30	4.50 ± 0.15	13.32 ± 2.48	> 60	> 60
T22I	0.49 ± 0.09	2.82 ± 0.16	2.53 ± 0.15	> 60	35.11 ± 9.50
E33A	0.45 ± 0.06	26.68 ± 4.00	41.45 ± 5.78	> 60	5.78 ± 2.44
D79N	0.56 ± 0.19	0.65 ± 0.07	0.70 ± 0.04	6.92 ± 1.85	0.80 ± 0.25
A107N	0.87 ± 0.09	1.99 ± 0.38	2.66 ± 0.39	12.18 ± 4.59	65.94 ± 8.50
R346S	0.45 ± 0.03	0.54 ± 0.04	0.66 ± 0.15	1.87 ± 0.45	28.24 ± 3.62
R380A	0.50 ± 0.13	8.16 ± 0.35	4.53 ± 0.13	26.44 ± 2.31	12.20 ± 0.87